

Robust Anti-swing Control for Unmanned Helicopter Slung-Load System with Prescribed Performance

SHAO Shuyi^{1,2}, LIU Nan¹, LI Chunru¹, CHEN Mou^{1*}

1. College of Automation Engineering, Nanjing University of Aeronautics and Astronautics, Nanjing 211106, P. R. China;

2. College of Aerospace Engineering, Nanjing University of Aeronautics and Astronautics, Nanjing 210016, P. R. China

(Received 22 March 2021; revised 10 April 2021; accepted 17 April 2021)

Abstract: A robust anti-swing control method based on the error transformation function is proposed, and the problem is handled for the unmanned helicopter slung-load system (HSLs) deviating from the equilibrium state due to the disturbances in the lifting process. First, the nonlinear model of unmanned HSLs is established. Second, the errors of swing angles are constructed by using the two ideal swing angle values and the actual swing angle values for the unmanned HSLs under flat flight, and the error transformation functions are investigated to guarantee that the errors of swing angles satisfy the prescribed performance. Third, the nonlinear disturbance observers are introduced to estimate the bounded disturbances, and the robust controllers of the unmanned HSLs, the velocity and the attitude subsystems are designed based on the prescribed performance method, the output of disturbance observer and the sliding mode backstepping strategy, respectively. Fourth, the Lyapunov function is developed to prove the stability of the closed-loop system. Finally, the simulation studies are shown to demonstrate the effectiveness of the control strategy.

Key words: unmanned helicopter slung-load system; prescribed performance; anti-swing control; disturbance observer; sliding mode controller

CLC number: V19

Document code: A

Article ID: 1005-1120(2021)02-0193-13

0 Introduction

The unmanned helicopter slung system is widely used in military transportation, disaster relief, etc., because of its capabilities of low altitude flight, fast loading and unloading of cargo, crossing obstacles and fast arriving at destination^[1]. In recent years, with the development and application of large and medium-sized unmanned helicopters in various countries, the volume and weight of lifting goods by unmanned helicopters are increasing, which makes the unmanned helicopter slung-load system (HSLs) becomes an important application use of unmanned helicopters^[2].

Compared with the unmanned HSLs, the external hanging load of the unmanned helicopter is in-

creased. The whole system becomes a highly coupled, underactuated, nonlinear system. The slung-load may oscillate due to the factors, like the maneuvering of the unmanned helicopter or the external disturbances. How to effectively control the unmanned helicopter to suppress load oscillation has become a research hotspot in the control field^[3]. Until now, many scholars have conducted many studies on the HSLs. For instance, in view of the influence of slung-load on the unmanned helicopter system, the load influence on various modes of the helicopter by direct balancing method in Refs.[4-5]. In Ref.[6], three dynamic equations of helicopter hoisting system were established, and the instruction smoothing technology was used to suppress load oscillation. Based on the flight dynamics model of the helicopter/crane coupling system, the balanc-

*Corresponding author, E-mail address: chenmou@nuaa.edu.cn.

How to cite this article: SHAO Shuyi, LIU Nan, LI Chunru, et al. Robust anti-swing control for unmanned helicopter slung-load system with prescribed performance[J]. Transactions of Nanjing University of Aeronautics and Astronautics, 2021, 38(2): 193-205.

<http://dx.doi.org/10.16356/j.1005-1120.2021.02.001>

ing and linearization of the coupling system were realized in Ref.[7], and the flight control law was designed to improve the operation stability characteristics of the helicopter/crane coupling system. To realize load oscillation suppression, a design strategy of the active disturbance rejection control was proposed based on the improved genetic algorithm in Ref.[8], which realized the on-line estimation of the parameter uncertainties and the external disturbances to reduce the control errors and achieve the load swing reduction. For the control of the helicopter trajectory tracking and the swing reduction, a nonlinear trajectory tracking controller (TTC) was designed by using the backstepping control strategy in Ref.[9], and the load oscillation suppression was realized through disturbance rejection delay feedback control. In Ref.[10], the unmanned HSLS was divided into the helicopter subsystem and the hanging subsystem, and the sliding mode controller and the swing reduction controller were designed to achieve the purpose of the load oscillation suppression. In order to achieve the load swing reduction, a nonlinear TTC was designed for the unmanned HSLS in Ref.[11]. In addition, many scholars have studied the four-rotor SLS and the bridge crane SLS, and a lot of significant research results were achieved in Refs.[12-13], which has reference significance for the research on the unmanned HSLSs.

Since the unmanned HSLS will be affected by external disturbances in the lifting process, it is necessary to deal with the disturbances in order to ensure the effectiveness of the designed controller. Among the existing disturbance rejection methods, the disturbance observer is one of the effective strategies to deal with external disturbances^[14-18]. For instance, for the attitude system of the variable swept-wing aircraft with external disturbances, the attitude control method was proposed based on the finite time disturbance observer and the fixed time disturbance observer in Ref.[14]. For the quadrotor system with external disturbances and uncertainties, an integral backstepping sliding mode control strategy based on the disturbance observer was proposed in

Ref.[15]. In Ref.[16], a sliding mode control method was proposed based on the disturbance observer for the nonlinear systems with disturbances. For the unmanned HSLS, the excessive load swing angle will affect the flight quality of the unmanned helicopter and even endanger the flight safety. Thus, it is necessary to consider the control of limited swing angle. There are generally three methods to deal with the output constraint control problems, including the obstacle Lyapunov function^[19], the funnel control method^[20] and the error transfer function method^[21-23]. Among them, the error transfer function method was widely used in dealing with the output constraint control problems. For example, for the TTC design problem of the small unmanned helicopter, a nonlinear TTC was designed by using the error transfer function method in Ref.[21], so that the tracking error can meet the prescribed performance. In Ref.[22], a distributed attitude cooperative control strategy was studied based on the prescribed performance method for a three degrees of freedom unmanned helicopter attitude constraint system with input saturation. A prescribed performance tracking controller was designed for the nonlinear systems with unknown control direction and input saturation.

Inspired by the literature mentioned above, the main contributions of this paper are as follows:

- (1) A disturbance observer is adopted to deal with the anti-disturbance problem.
- (2) A robust control method is designed based on the error transfer function for the unmanned HSLS with swing angle constraint and disturbance.
- (3) The control scheme can guarantee that all signals in the closed-loop system are bounded and the load swing angle error can meet the prescribed performance.

The sections of this paper are as follows: Section 1 describes the coupling nonlinear dynamic model of the unmanned HSLS and the physical meaning of each parameter, and then gives the system control target and control flow chart; in section 2, the controller of lifting subsystem, velocity sub-

system and attitude subsystem are designed; section 3 proves the stability of the closed-loop system; section 4 presents the numerical simulation results and analysis; and section 5 draws conclusions of the study.

1 Unmanned Helicopter Slung-Load System Model

In this section, a full-state coupling nonlinear mathematical model of the unmanned HSLS is established on the basis of the medium unmanned helicopter flying flat at a low speed. The following assumptions are given^[10, 21]:

(1) The ground coordinate system is adopted as the inertial coordinate system.

(2) The mass distribution of the unmanned helicopter is uniform, and the center of mass does not change.

(3) The unmanned helicopter is strictly symmetrical, and the speed of the main rotor is unchanged.

(4) The rope is a rigid body, weightless and in a tight state at all times.

(5) The hanging point is directly below the center of the mass of the unmanned helicopter.

(6) The swing angle of the hanging load oscillates at a small angle.

Under the assumptions above, the dynamic equation of the medium-size unmanned helicopter is given, and it can be described as^[21]

$$\begin{cases} \dot{\mathbf{r}} = \mathbf{\Gamma} \\ m_h \dot{\mathbf{\Gamma}} = m_h \mathbf{G} - \mathbf{R}_b^g \mathbf{T} \\ \dot{\boldsymbol{\theta}} = \mathbf{H} \boldsymbol{\Omega} \\ \mathbf{J} \dot{\boldsymbol{\Omega}} = -\boldsymbol{\Omega} \times \mathbf{J} \boldsymbol{\Omega} + \boldsymbol{\Sigma} \end{cases} \quad (1)$$

where $\mathbf{r} = [x, y, z]^T$ and $\mathbf{\Gamma} = [u, v, w]^T$ are the position and the velocity vectors of the unmanned helicopter under the inertial frame, respectively; $\boldsymbol{\theta} = [\phi, \theta, \psi]^T$ and $\boldsymbol{\Omega} = [p, q, r]^T$ the three Euler angles of the unmanned helicopter in the inertial frame and the angular velocity in the body coordinate system, respectively; $\mathbf{T} = [0, 0, T_{mr}]^T$ and $\boldsymbol{\Sigma} = [L, M, N]^T$ the input force and the torque vectors for the un-

manned helicopter, respectively; T_{mr} represents the pull of the main rotor; \mathbf{H} the transformation matrix from the attitude angular velocity to the Euler angular velocity, and \mathbf{R}_b^g the transformation matrix from the body coordinate system to the ground coordinate system; $\mathbf{G} = [0, 0, g]^T$ the gravitational acceleration vector, and g is the gravitational acceleration; $\mathbf{J} = [J_{xx}, J_{yy}, J_{zz}]^T$ the vector of the rotational inertia, and m_h the mass of the unmanned helicopter.

The slung-load is added on the basis of the model (1), and the output of the lifting subsystem is defined as the back swing angle θ_1 of the load and the side swing angle ϕ_1 . Then, the displacement of the load relative to the hanging point is defined as \mathbf{P}_1 , and the specific form is as follows^[10]

$$\mathbf{P}_1 = [x_1, y_1, z_1]^T = [-l \cos \phi_1 \sin \theta_1, -l \sin \phi_1, l \cos \phi_1 \cos \theta_1]^T \quad (2)$$

where l is the length of the rope. Displacement of load relative to the helicopter center of mass \mathbf{P}_L is given by

$$\mathbf{P}_L = \mathbf{P}_1 + \mathbf{P}_h \quad (3)$$

where $\mathbf{P}_h = [0, 0, l_h]^T$ is the displacement of the hanging point to the center of mass of the helicopter, and l_h the distance between the hanging point and the center of mass of the helicopter.

Then the velocity of the slung-load under the inertial frame can be written as^[9, 10]

$$\mathbf{V}_1 = \mathbf{\Gamma} + \dot{\mathbf{P}}_L + \boldsymbol{\Omega} \times \mathbf{P}_L \quad (4)$$

Furthermore, the force F_1 of the slung-load acting on a helicopter, and the moment M_1 can be represented as

$$\begin{cases} F_1 = -m_1 \dot{\mathbf{V}}_1 + m_1 \mathbf{G} + \mathbf{D} \\ \mathbf{M}_1 = \mathbf{P}_h \times F_1 \end{cases} \quad (5)$$

where m_1 is the load mass; $\mathbf{D} = 0.5 \rho s_1 \|\mathbf{V}_1\| \mathbf{V}_1$ the air resistance of the load; ρ the damping coefficient; and s_1 the equivalent windward area of the load.

In addition, the equilibrium equation by suspension point moment is given as follows^[9, 10]

$$\mathbf{P}_L \times F_1 = 0 \quad (6)$$

The dynamic model of the load can be obtained by solving Eq.(6), and one can obtain

$$\mathbf{A} = F(\mathbf{A}) + G(\mathbf{A}) \mathbf{P} \quad (7)$$

where $\mathbf{A} = [\dot{\theta}_1, \dot{\phi}_1]^T$ is the swing angle vector of the

slung-load; and $P = [\dot{u}, \dot{v}]^T$ the input for the slung-load subsystem. $F(\mathbf{A})$ and $G(\mathbf{A})$ can be written as^[10]

$$F(\mathbf{A}) = \begin{bmatrix} l^2 S_{\phi_1} C_{\phi_1} S_{\theta_1} & l^2 C_{\theta_1} \\ -l^2 C_{\phi_1}^2 & 0 \end{bmatrix}^{-1} \begin{bmatrix} A \\ B \end{bmatrix}$$

$$G(\mathbf{A}) = \begin{bmatrix} l^2 S_{\phi_1} C_{\phi_1} S_{\theta_1} & l^2 C_{\theta_1} \\ -l^2 C_{\phi_1}^2 & 0 \end{bmatrix}^{-1} \begin{bmatrix} 0 & z_1 \\ -z_1 & 0 \end{bmatrix}$$

$$A = -k \|V_1\| (y_1 (\dot{\phi}_1 l S_{\phi_1} C_{\theta_1} + \dot{\theta}_1 l C_{\phi_1} S_{\theta_1}) - z_1 (v - \dot{\phi}_1 l C_{\phi_1})) + 2\dot{\phi}_1 \dot{\theta}_1 l^2 S_{\phi_1}^2 S_{\theta_1} + y_1 g - \dot{\theta}_1^2 l^2 S_{\phi_1} C_{\phi_1} C_{\theta_1}$$

$$B = k \|V_1\| z_1 (u + \dot{\phi}_1 l S_{\phi_1} S_{\theta_1} - \dot{\theta}_1 l C_{\phi_1} C_{\theta_1} - x_1 (-\dot{\phi}_1 l S_{\phi_1} C_{\theta_1} - \dot{\theta}_1 l C_{\phi_1} S_{\theta_1})) - x_1 g - 2\dot{\phi}_1 \dot{\theta}_1 l^2 C_{\phi_1} S_{\phi_1}$$

where $k = 0.5\rho s$ is the equivalent damping coefficient of the load; S_{ϕ_1} , C_{ϕ_1} , S_{θ_1} and C_{θ_1} are the short forms for $\sin\phi_1$, $\cos\phi_1$, $\sin\theta_1$ and $\cos\theta_1$, respectively. The swing angle of the lifting load is in $[-\pi/2, \pi/2]$, thus $G(\mathbf{A})$ is reversible. From Eq.(7), the reaction force F_1 and moment M_1 of the load on the helicopter can be inversely solved.

The coupling nonlinear model of the unmanned HSLs under the effect of disturbances is shown as follows

$$\begin{cases} \dot{\mathbf{A}} = F(\mathbf{A}) + G(\mathbf{A})\mathbf{P} + d_1 \\ \dot{r} = \Gamma \\ m_h \dot{\Gamma} = m_h G - R_b^k T + F_1 + d_2 \\ \dot{\Theta} = H\Omega \\ J\dot{\Omega} = -\Omega \times J\Omega + \Sigma + M_1 + d_3 \end{cases} \quad (8)$$

where $F_1 = [F_{1x}, F_{1y}, F_{1z}]^T$, F_{1x} , F_{1y} and F_{1z} are the components of F_1 along the coordinate axis x , y and z , respectively; $M_1 = [M_{1x}, M_{1y}, 0]^T$, M_{1x} , M_{1y} are the components of M_1 along the coordinate axis x and y , respectively; $d_i \in \mathbb{R}^3$, $i = 1, 2, 3$ the external disturbances.

The control objectives of this paper are as follows: According to the load stability swing angle of the unmanned HSLs under the states of balance θ_{ld} and ϕ_{ld} , a robust anti-swing controller is designed for the slung-load subsystem to make the swing angles converge to a small neighborhood near the desired swing angles. Then a robust controller is designed to control the speed and attitude angles of the helicopter. Finally, the unmanned helicopter is in the state of flat flight, while the load swing angles are in the small neighborhood of the target swing angles. On the basis of the control objectives, the control structure diagram of this paper is shown in Fig.1^[10].

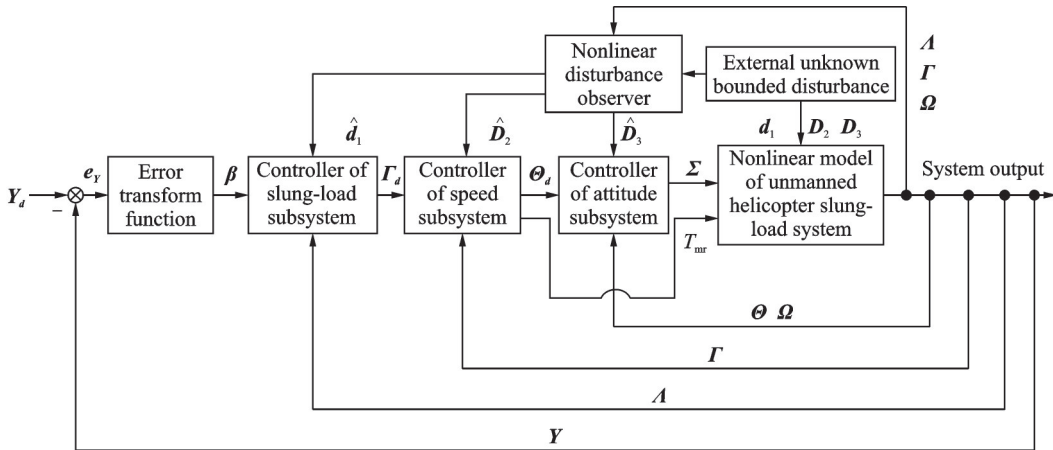


Fig.1 Unmanned HSLs controller design

2 Unmanned Helicopter Slung-Load System Controller Design

For the convenience of the subsequent controller design, the following assumptions and lemmas are given.

Assumption 1^[21] The helicopter pitch angle ϕ and the roll angle θ satisfy the following inequalities that $-\frac{\pi}{2} < \phi < \frac{\pi}{2}$ and $-\frac{\pi}{2} < \theta < \frac{\pi}{2}$.

Assumption 2^[21] All states of the system are measurable.

Assumption 3^[21] For the external disturbance $d_i \in \mathbf{R}^3$, $i = 1, 2, 3$, assume that there are positive constants δ_i ensure $\|\dot{d}_i\| \leq \delta_i$, where $\|\cdot\|$ represents the 2-norm of a vector.

Assumption 4^[15, 21] The desired signal $\mathbf{F}_d(t)$ of the speed subsystem and the desired signal $\mathbf{\Theta}_d$ of the attitude subsystem are sufficiently smooth functions and satisfy that $\mathbf{F}_d \in \mathbf{M}_F$, $\mathbf{\Theta}_d \in \mathbf{M}_\Theta$, and the functions satisfy that $\mathbf{M}_F = \{(\mathbf{F}_d, \dot{\mathbf{F}}_d, \ddot{\mathbf{F}}_d): \|\mathbf{F}_d\|^2 + \|\dot{\mathbf{F}}_d\|^2 + \|\ddot{\mathbf{F}}_d\|^2 \leq o_1\}$, and $\mathbf{M}_\Theta = \{(\mathbf{\Theta}_d, \dot{\mathbf{\Theta}}_d, \ddot{\mathbf{\Theta}}_d): \|\mathbf{\Theta}_d\|^2 + \|\dot{\mathbf{\Theta}}_d\|^2 + \|\ddot{\mathbf{\Theta}}_d\|^2 \leq o_2\}$, where the parameter o_1 and o_2 are unknown positive constants.

Lemma 1^[17] For a bounded system with initial conditions at time zero, if there exists a continuous positive definite Lyapunov function, one has

$$\pi_1(\|x\|) \leq V(x) \leq \pi_2(\|x\|) \quad (9)$$

and

$$\dot{V}(x) \leq -C_1 V(x) + C_2 \quad (10)$$

then the system solution $x(t)$ is ultimately uniformly bounded, where π_1 and π_2 are the K_∞ class function, C_1 and C_2 the positive constants.

2.1 Slung-load subsystem controller design

The load swing angle error vector is defined as $e_Y = Y - Y_d = [e_{Y1}, e_{Y2}]^T$, where the signals can be described as $Y = [\theta, \phi]^T$ and $Y_d = [\theta_d, \phi_d]^T$, e_{Yi} is the i th element of e_Y . To realize the restricted control of load swing angles, it is necessary to constrain the swing angle errors. The specific form is given as follows

$$-\lambda_{1i}\chi_i(t) < e_{Yi} < \lambda_{2i}\chi_i(t) \quad i = 1, 2 \quad (11)$$

where $\lambda_{1i}, \lambda_{2i} \in (0, 1]$ are the design parameters; $\chi_i(t)$ is the prescribed performance function, and the expression can be written as^[21]

$$\chi_i(t) = (\chi_{i0} - \chi_{i\infty})\exp(-\delta_i t) + \chi_{i\infty} \quad (12)$$

By designing the parameters $\delta_i > 0$ and $\chi_{i0} > \chi_{i\infty} > 0$, the steady-state and the transient performance of the swing angle error can be constrained. According to the above definition, we have $\chi_i(0) = \chi_{i0}$, $\lim_{t \rightarrow \infty} \chi_i(t) = \chi_{i\infty}$, where $\chi_i(t)$ is a smooth decreasing function.

To obtain the control performance above, an error transfer function is introduced to convert the constrained inequality into an unconstrained form^[21]

$$\beta_i = Q\left(\frac{e_{Yi}(t)}{\chi_i(t)}\right) \quad i = 1, 2 \quad (13)$$

where β_i is the variable of transformed error, and $Q(\cdot)$ satisfies the following properties^[21]

$$\begin{cases} Q(\cdot): (-\lambda_{1i}, \lambda_{2i}) \rightarrow (-\infty, \infty) \\ \lim_{e_{Yi}/\chi_i \rightarrow -\lambda_{1i}} Q(\cdot) = -\infty \\ \lim_{e_{Yi}/\chi_i \rightarrow \lambda_{2i}} Q(\cdot) = \infty \end{cases} \quad (14)$$

It can be known from Eq.(14) that β_i can be utilize to ensure the predetermined transient and steady-state performance. Thus, the control objectives of the system can be converted to that the error transfer variable β_i is bounded under a designed controller^[21-23], then the swing angle error can meet the prescribed performance in Eq.(11).

Considering the effect of external disturbance d_1 , the lifting subsystem model can be written as

$$\begin{cases} \dot{Y} = \mathbf{A} \\ \dot{\Lambda} = F(\Lambda) + G(\Lambda)\mathbf{P} + d_1 \end{cases} \quad (15)$$

To ensure that the swing angle of the slung-load subsystem can be converged quickly and stabilized in the small neighborhood near the desired value, the following design of the swing angle controller is given based on the prescribed performance function.

According to the result in Ref.[21], the transfer error β_i is written as

$$\beta_i = \left[1 - \alpha\left(\frac{e_{Yi}(0)}{\chi_i(0)}\right)\right] \frac{e_{Yi}(t)/\chi_i(t)}{\lambda_{1i} + e_{Yi}(t)/\chi_i(t)} + \alpha\left(\frac{e_{Yi}(0)}{\chi_i(0)}\right) \frac{e_{Yi}(t)/\chi_i(t)}{\lambda_{2i} + e_{Yi}(t)/\chi_i(t)} \quad (16)$$

Then, we define that $\alpha_i = \alpha(e_{Yi}(0)/\chi_i(0))$ and $\alpha_i = \begin{cases} 1 & e_{Yi}(0) \geq 0 \\ 0 & e_{Yi}(0) < 0 \end{cases}$. Thus, the transfer error can be written as

$$\beta_i = (1 - \alpha_i)e_{Yi}(t)/(\lambda_{1i}\chi_i(t) + e_{Yi}(t)) + \alpha_i e_{Yi}(t)/(\lambda_{2i}\chi_i(t) + e_{Yi}(t)) \quad (17)$$

The derivative of β_i can be obtained as follows

$$\begin{aligned} \dot{\beta}_i &= (1 - \alpha_i) \cdot \\ & \frac{\dot{e}_{Y_i}(t) (\lambda_{1i} \chi_i(t) + e_{Y_i}(t)) - e_{Y_i}(t) (\lambda_{1i} \dot{\chi}_i(t) + \dot{e}_{Y_i}(t))}{(\lambda_{1i} \chi_i(t) + e_{Y_i}(t))^2} + \\ & \alpha_i \frac{\dot{e}_{Y_i}(t) (\lambda_{2i} \chi_i(t) + e_{Y_i}(t)) - e_{Y_i}(t) (\lambda_{2i} \dot{\chi}_i(t) + \dot{e}_{Y_i}(t))}{(\lambda_{2i} \chi_i(t) + e_{Y_i}(t))^2} = \\ & \dot{e}_{Y_i}(t) \Pi_i \chi_i(t) - e_{Y_i}(t) \Pi_i \dot{\chi}_i(t) \end{aligned} \quad (18)$$

where $\Pi_i = (1 - \alpha_i) \lambda_{1i} / (\lambda_{1i} \chi_i(t) + e_{Y_i}(t))^2 + \alpha_i \lambda_{2i} / (\lambda_{2i} \chi_i(t) + e_{Y_i}(t))^2$.

It can define that $\beta = [\beta_1, \beta_2]^T$, $\Pi = \text{diag} \{ \Pi_1, \Pi_2 \}$ and $\chi = \text{diag} \{ \chi_1, \chi_2 \}$, then one has

$$\dot{\beta} = \chi \Pi \dot{e}_Y - \dot{\chi} \Pi e_Y \quad (19)$$

Considering the error signal $e_Y = Y - Y_d$, the slung-load subsystem model (15) can be transformed into the following form

$$\begin{cases} \dot{\beta} = \chi \Pi (\mathbf{A} - \dot{Y}_d) - \dot{\chi} \Pi e_Y \\ \dot{\mathbf{A}} = F(\mathbf{A}) + G(\mathbf{A}) \mathbf{P} + d_1 \end{cases} \quad (20)$$

where χ , Π and e_Y are all known and can be used in the controller design.

To estimate the unknown disturbance in the lifting subsystem, a nonlinear disturbance observer of the following form is designed by^[14]

$$\begin{cases} \dot{\hat{d}}_1 = Z_1 + P_1(\mathbf{A}) \\ \dot{Z}_1 = -L_1(Z_1 + P_1(\mathbf{A})) + F(\mathbf{A}) + G(\mathbf{A}) \mathbf{P} \end{cases} \quad (21)$$

where $Z_1 \in \mathbf{R}^3$ is the internal variable of the nonlinear disturbance observer; $\hat{d}_1 \in \mathbf{R}^3$ the estimated value of disturbance d_1 ; $P_1(\mathbf{A}) \in \mathbf{R}^3$ the function to be designed with respect to the variable \mathbf{A} ; $L_1 \in \mathbf{R}^{3 \times 3}$ the gain function and $L_1 = \partial P_1(\mathbf{A}) / \partial \mathbf{A}$.

The disturbance observer error is defined as

$$\bar{d}_1 = \hat{d}_1 - d_1 \quad (22)$$

From Eq.(22), one has

$$\begin{aligned} \dot{\bar{d}}_1 &= -L_1 Z_1 - L_1 (P_1(\mathbf{A}) + F(\mathbf{A}) + G(\mathbf{A}) \mathbf{P}) + \\ & L_1 (F(\mathbf{A}) + G(\mathbf{A}) \mathbf{P} + d_1) - \dot{\hat{d}}_1 = \\ & -L_1 \bar{d}_1 - \dot{\hat{d}}_1 \end{aligned} \quad (23)$$

The Lyapunov function is designed as

$$V_1 = \frac{1}{2} \bar{d}_1^T \bar{d}_1 \quad (24)$$

According to Assumption 3, and Eqs.(23, 24) can be written as

$$\begin{aligned} \dot{V}_1 &= \bar{d}_1^T (-L_1 \bar{d}_1 - \dot{\hat{d}}_1) \leq \\ & -\bar{d}_1^T (L_1 - 0.5I_2) \bar{d}_1 + 0.5\delta_1^2 \end{aligned} \quad (25)$$

where I_2 is the second-order identity matrix. Then,

the following backstepping method is used to design the slung-load subsystem controller.

Define the constrained variables ω_1 and ω_2 as

$$\begin{cases} \omega_1 = \beta \\ \omega_2 = \mathbf{A} - \mathbf{E}_d \end{cases} \quad (26)$$

where \mathbf{E}_d is the virtual control law to be designed.

On the basis of Eqs. (20, 26), it can be deduced as

$$\begin{aligned} \dot{\omega}_1 &= \chi \Pi (\omega_2 + \mathbf{E}_d - \dot{Y}_d) - \dot{\chi} \Pi e_Y = \\ & \chi \Pi \mathbf{E}_d + \chi \Pi \omega_2 - \chi \Pi \dot{Y}_d - \dot{\chi} \Pi e_Y \end{aligned} \quad (27)$$

Furthermore, the virtual control law is designed as

$$\mathbf{E}_d = (\chi \Pi)^{-1} (\chi \Pi \dot{Y}_d + \dot{\chi} \Pi e_Y - k_1 \omega_1) \quad (28)$$

where $k_1 = k_1^T > 0$ is the design parameter matrix.

Substituting Eq.(28) into Eq.(27), one has

$$\dot{\omega}_1 = -k_1 \omega_1 + \chi \Pi \omega_2 \quad (29)$$

Combining Eq.(20) and Eq.(26), one has

$$\dot{\omega}_2 = F(\mathbf{A}) + G(\mathbf{A}) \mathbf{P} + d_1 - \dot{\mathbf{E}}_d \quad (30)$$

Then, the slung-load subsystem control law is designed as

$$\begin{aligned} \mathbf{P} &= G^{-1}(\mathbf{A}) (-F(\mathbf{A}) + \dot{\mathbf{E}}_d - \hat{d}_1 - k_2 \omega_2 + \\ & (\chi \Pi)^T \omega_1) \end{aligned} \quad (31)$$

where $k_2 = k_2^T > 0$ is the matrix to be designed;

$\mathbf{P} = [\dot{u}_d, \dot{v}_d]^T$ the helicopter acceleration measure required for the oscillation reduction. The target velocity is obtained by integrating \mathbf{P} , $[u_d, v_d]^T$, will be used in the controller design of the speed subsystem.

Substituting Eq. (31) into Eq. (30), one can obtain

$$\dot{\omega}_2 = -k_2 \omega_2 - (\chi \Pi)^T \omega_1 - \bar{d}_1 \quad (32)$$

For the slung-load subsystem, the Lyapunov function can be designed as

$$V_2 = 0.5 \omega_1^T \omega_1 + 0.5 \omega_2^T \omega_2 \quad (33)$$

Considering Eqs.(29, 32, 33), we have

$$\begin{aligned} \dot{V}_2 &= \omega_1^T \dot{\omega}_1 + \omega_2^T \dot{\omega}_2 = \\ & -\omega_1^T k_1 \omega_1 + \omega_1^T \chi \Pi \omega_2 - \omega_2^T k_2 \omega_2 - \\ & \omega_2^T (\chi \Pi)^T \omega_1 + \omega_2^T \bar{d}_1 = \\ & -\omega_1^T k_1 \omega_1 - \omega_2^T k_2 \omega_2 + \omega_2^T \bar{d}_1 \end{aligned} \quad (34)$$

2.2 Speed subsystem controller design

On the basis of the model (8) for the unmanned HSLS, the affine nonlinear model of the velocity subsystem can be obtained as

$$\dot{\mathbf{I}} = \mathbf{f}(\mathbf{I}) + \mathbf{g}(\mathbf{I})\mathbf{T} + \mathbf{D}_2 \quad (35)$$

where

$$\mathbf{T} = \begin{bmatrix} -T_{mr}(\cos\phi\sin\theta\cos\psi + \sin\phi\sin\psi) \\ T_{mr}(\cos\phi\sin\theta\sin\psi - \sin\phi\cos\psi) \\ -T_{mr}\cos\phi\cos\theta \end{bmatrix}$$

$$\mathbf{f}(\mathbf{I}) = \begin{bmatrix} F_{11}/m_h \\ F_{12}/m_h \\ \mathbf{g} + F_{13}/m_h \end{bmatrix}$$

$$\mathbf{D}_2 = \frac{\mathbf{d}_2}{m_h} = [D_{21}, D_{22}, D_{23}]^T$$

$$\mathbf{g}(\mathbf{I}) = \text{diag}\{1/m_h, 1/m_h, 1/m_h\}$$

To estimate the unknown disturbances in the velocity subsystem, a nonlinear disturbance observer consistent with Eq.(21) is designed by

$$\begin{cases} \dot{\hat{\mathbf{D}}}_2 = \mathbf{Z}_2 + \mathbf{P}_2(\mathbf{I}) \\ \dot{\mathbf{Z}}_2 = -\mathbf{L}_2(\mathbf{Z}_2 + \mathbf{P}_2(\mathbf{I}) + \mathbf{f}(\mathbf{I}) + \mathbf{g}(\mathbf{I})\mathbf{T}) \end{cases} \quad (36)$$

where $\mathbf{Z}_2 \in \mathbf{R}^3$ is the internal variable of the nonlinear disturbance observer; $\hat{\mathbf{D}}_2 \in \mathbf{R}^3$ the estimated value of disturbance \mathbf{D}_2 ; $\mathbf{P}_2(\mathbf{I}) \in \mathbf{R}^3$ the function to be designed with respect to the variable \mathbf{I} , and $\mathbf{L}_2 \in \mathbf{R}^{3 \times 3}$ the gain function and $\mathbf{L}_2 = \partial \mathbf{P}_2(\mathbf{I}) / \partial \mathbf{I}$.

The disturbance observer error is defined as

$$\bar{\mathbf{D}}_2 = \hat{\mathbf{D}}_2 - \mathbf{D}_2 \quad (37)$$

From Eq.(37), the error of the disturbance observer can be obtained as

$$\dot{\bar{\mathbf{D}}}_2 = -\mathbf{L}_2 \bar{\mathbf{D}}_2 - \dot{\mathbf{D}}_2 \quad (38)$$

The form of Lyapunov function is designed by

$$\mathbf{V}_3 = 0.5 \bar{\mathbf{D}}_2^T \bar{\mathbf{D}}_2 \quad (39)$$

Substituting Eq.(38) into Eq.(39), one can obtain

$$\dot{\mathbf{V}}_3 \leq -\bar{\mathbf{D}}_2^T (\mathbf{L}_2 - 0.5\mathbf{I}_3) \bar{\mathbf{D}}_2 + 0.5\bar{\delta}_2^2 \quad (40)$$

where \mathbf{I}_3 is the third-order identity matrix, and $\bar{\delta}_2 = \delta_2/m_h$.

Then, the tracking error vector of the helicopter velocity is defined as

$$\mathbf{e}_r = \mathbf{I} - \mathbf{I}_d = [u - u_d, v - v_d, w - w_d]^T \quad (41)$$

where $\mathbf{I}_d = [u_d, v_d, w_d]^T \in \mathbf{R}^{3 \times 1}$ is the tracking speed of the velocity subsystem; $[\dot{u}_d, \dot{v}_d]^T = \mathbf{P}$, and w_d is a known signal.

The Lyapunov function is given as

$$\mathbf{V}_4 = 0.5 \mathbf{e}_r^T \mathbf{e}_r \quad (42)$$

The first derivative of Eq.(42) can be described as

$$\dot{\mathbf{V}}_4 = \mathbf{e}_r^T (\dot{\mathbf{I}} - \dot{\mathbf{I}}_d) \quad (43)$$

where $\dot{\mathbf{I}}_d = [\dot{u}_d, \dot{v}_d, \dot{w}_d]^T \in \mathbf{R}^{3 \times 1}$, and \dot{w}_d is quantitative. Further combining Eq.(35), one has

$$\dot{\mathbf{V}}_4 = \mathbf{e}_r^T (\mathbf{f}(\mathbf{I}) + \mathbf{g}(\mathbf{I})\mathbf{T} + \mathbf{D}_2 - \dot{\mathbf{I}}_d) \quad (44)$$

The control law of the speed subsystem is designed as

$$\mathbf{T} = \mathbf{g}(\mathbf{I})^{-1} (-\mathbf{f}(\mathbf{I}) + \dot{\mathbf{I}}_d - \mathbf{k}_3 \mathbf{e}_r - \hat{\mathbf{D}}_2) \quad (45)$$

where $\mathbf{k}_3 = \mathbf{k}_3^T$ is a positive definite symmetric matrix to be designed. Substituting Eq.(45) into Eq.(44), one can obtain

$$\dot{\mathbf{V}}_4 = -\mathbf{k}_3 \mathbf{e}_r^T \mathbf{e}_r - \mathbf{e}_r^T \bar{\mathbf{D}}_2 \quad (46)$$

The attitude angles and the pull force of the helicopter can be solved by the control quantities as follows^[21]

$$\begin{cases} \theta_d = \arctan((T_1 \cos \psi_d + T_2 \sin \psi_d) / T_3) \\ \phi_d = \arctan(\cos \theta_d (T_1 \sin \psi_d - T_2 \cos \psi_d) / T_3) \\ T_{mr} = -T_3 / (\cos \phi_d \cos \theta_d) \end{cases} \quad (47)$$

where the yaw angle ψ_d is known.

According to Eq.(47), the attitude tracking signal of the attitude subsystem is $\boldsymbol{\Theta}_d = [\phi_d, \theta_d, \psi_d]^T$, and the signal will be used in the controller design of the attitude subsystem.

2.3 Attitude subsystem controller design

On the basis of the model (8) of the unmanned HLSL, the affine nonlinear mathematical model of the attitude subsystem for the unmanned helicopter can be written as

$$\begin{cases} \dot{\boldsymbol{\Theta}} = \mathbf{H}\boldsymbol{\Omega} \\ \dot{\boldsymbol{\Omega}} = \mathbf{f}(\boldsymbol{\Omega}) + \mathbf{g}(\boldsymbol{\Omega})\boldsymbol{\Sigma} + \mathbf{D}_3 \end{cases} \quad (48)$$

where

$$\mathbf{H} = \begin{bmatrix} 1 & \sin\phi \tan\theta & \cos\phi \tan\theta \\ 0 & \cos\phi & -\sin\phi \\ 0 & \sin\phi / \cos\theta & \cos\phi / \cos\theta \end{bmatrix}$$

$$\mathbf{f}(\boldsymbol{\Omega}) = \begin{bmatrix} (J_{yy} - J_{zz})qr / J_{xx} + M_{hr} / J_{xx} \\ (J_{zz} - J_{xx})pr / J_{yy} + M_{hy} / J_{yy} \\ (J_{xx} - J_{yy})pr / J_{zz} + M_{hz} / J_{zz} \end{bmatrix}$$

$$\mathbf{g}(\boldsymbol{\Omega}) = \text{diag}\{1/J_{xx}, 1/J_{yy}, 1/J_{zz}\}$$

$$\mathbf{D}_3 = \mathbf{J}^{-1} \mathbf{d}_3 = [D_{31}, D_{32}, D_{33}]^T$$

To estimate the unknown disturbance in the attitude subsystem, a nonlinear disturbance observer consistent with the form of Eq.(21) is designed as

$$\begin{cases} \hat{D}_3 = Z_3 + P_3(\boldsymbol{\Omega}) \\ \dot{Z}_3 = -L_3(Z_3 + P_3(\boldsymbol{\Omega}) + f(\boldsymbol{\Omega}) + g(\boldsymbol{\Omega})\boldsymbol{\Sigma}) \end{cases} \quad (49)$$

where $Z_3 \in \mathbf{R}^3$ is the internal variable of the nonlinear disturbance observer; $\hat{D}_3 \in \mathbf{R}^3$ the estimated value of disturbance D_3 ; $P_3(\boldsymbol{\Omega}) \in \mathbf{R}^3$ the function to be designed with respect to the variable $\boldsymbol{\Omega}$; $L_3 \in \mathbf{R}^{3 \times 3}$ the gain function and $L_3 = \partial P_3(\boldsymbol{\Omega}) / \partial \boldsymbol{\Omega}$.

The disturbance observer error is defined as

$$\bar{D}_3 = \hat{D}_3 - D_3 \quad (50)$$

By taking the derivative of Eq.(50), we can have the error dynamic as

$$\dot{\bar{D}}_3 = -L_3 \bar{D}_3 - \dot{D}_3 \quad (51)$$

The Lyapunov function is designed as

$$V_5 = 0.5 \bar{D}_3^T \bar{D}_3 \quad (52)$$

According to Assumption 2, and Eqs.(50, 52), one has

$$\dot{V}_5 \leq -\bar{D}_3^T (L_3 - 0.5I_3) \bar{D}_3 + 0.5\bar{\delta}_3^2 \quad (53)$$

where $\bar{\delta}_3 = \|J^{-1}\| \delta_3$.

The attitude error vectors of the helicopter are defined as

$$\begin{cases} \mathbf{e}_\theta = \boldsymbol{\Theta} - \boldsymbol{\Theta}_d \\ \mathbf{e}_\Omega = \boldsymbol{\Omega} - \boldsymbol{\Omega}_d \end{cases} \quad (54)$$

where $\boldsymbol{\Theta}_d = [\phi_d, \theta_d, \psi_d]^T$ is the tracking signal for the attitude system; and $\boldsymbol{\Omega}_d$ the virtual control law.

In order to avoid directly using the derivatives of the signals $\boldsymbol{\Theta}_d$ and $\boldsymbol{\Omega}_d$ in the subsequent controller design, the first order filter is introduced, and the variables ζ_θ and ζ_Ω can be expressed as

$$\begin{cases} \mu_\theta \dot{\zeta}_\theta + \zeta_\theta = \boldsymbol{\Theta}_d & \zeta_\theta(0) = \boldsymbol{\Theta}_d(0) \\ \mu_\Omega \dot{\zeta}_\Omega + \zeta_\Omega = \boldsymbol{\Omega}_d & \zeta_\Omega(0) = \boldsymbol{\Omega}_d(0) \end{cases} \quad (55)$$

where μ_θ and μ_Ω are the filter time constants. Define the filter errors as

$$\begin{cases} e_{\zeta_\theta} = \zeta_\theta - \boldsymbol{\Theta}_d \\ e_{\zeta_\Omega} = \zeta_\Omega - \boldsymbol{\Omega}_d \end{cases} \quad (56)$$

The derivative of Eq.(56) is obtained as follows

$$\begin{cases} \dot{e}_{\zeta_\theta} = \dot{\zeta}_\theta - \dot{\boldsymbol{\Theta}}_d = -e_{\zeta_\theta} / \mu_\theta - \dot{\boldsymbol{\Theta}}_d \\ \dot{e}_{\zeta_\Omega} = \dot{\zeta}_\Omega - \dot{\boldsymbol{\Omega}}_d = -e_{\zeta_\Omega} / \mu_\Omega - \dot{\boldsymbol{\Omega}}_d \end{cases} \quad (57)$$

where $\begin{cases} \dot{\boldsymbol{\Theta}}_d = M_2(\ddot{\boldsymbol{\Gamma}}_d, \dot{\boldsymbol{\Gamma}}_d, \boldsymbol{\Gamma}_d, \dot{\boldsymbol{\theta}}) \\ \dot{\boldsymbol{\Omega}}_d = M_3(\ddot{\boldsymbol{\Gamma}}_d, \dot{\boldsymbol{\Gamma}}_d, \boldsymbol{\Gamma}_d, \dot{\boldsymbol{\theta}}, \dot{\boldsymbol{\phi}}, \dot{\boldsymbol{\Theta}}_d) \end{cases}$.

The functions $M_2(\ddot{\boldsymbol{\Gamma}}_d, \dot{\boldsymbol{\Gamma}}_d, \boldsymbol{\Gamma}_d, \dot{\boldsymbol{\theta}})$ and

$M_3(\ddot{\boldsymbol{\Gamma}}_d, \dot{\boldsymbol{\Gamma}}_d, \boldsymbol{\Gamma}_d, \dot{\boldsymbol{\theta}}, \dot{\boldsymbol{\phi}}, \dot{\boldsymbol{\Theta}}_d)$ are fully smooth in the set $\mathcal{D}_2(\ddot{\boldsymbol{\Gamma}}_d, \dot{\boldsymbol{\Gamma}}_d, \boldsymbol{\Gamma}_d, \dot{\boldsymbol{\theta}})$ and $\mathcal{D}_3(\ddot{\boldsymbol{\Gamma}}_d, \dot{\boldsymbol{\Gamma}}_d, \boldsymbol{\Gamma}_d, \dot{\boldsymbol{\theta}}, \dot{\boldsymbol{\phi}}, \dot{\boldsymbol{\Theta}}_d)$, the sets $\mathcal{D}_2(\cdot)$ and $\mathcal{D}_3(\cdot)$ are compact sets, then $M_2(\cdot)$ and $M_3(\cdot)$ are bounded in compact sets $\mathcal{D}_2(\cdot)$ and $\mathcal{D}_3(\cdot)$ ^[21,24]. Then, we have

$$\|M_2(\cdot)\| \leq \bar{\boldsymbol{\Theta}}_d, \quad \|M_3(\cdot)\| \leq \bar{\boldsymbol{\Omega}}_d \quad (58)$$

and

$$\dot{\mathbf{e}}_\theta = H\mathbf{e}_\theta + H\boldsymbol{\Omega}_d - \dot{\boldsymbol{\Theta}}_d \quad (59)$$

The virtual control law is designed as

$$\boldsymbol{\Omega}_d = H^{-1}(\dot{\zeta}_\theta - k_4 \mathbf{e}_\theta) \quad (60)$$

where $k_4 > 0$ is the parameter to be designed.

Substituting Eq.(60) into Eq.(59), it can be obtain

$$\dot{\mathbf{e}}_\theta = H\mathbf{e}_\theta - k_4 \mathbf{e}_\theta + \dot{e}_{\zeta_\theta} \quad (61)$$

Define the sliding surfaces^[10]

$$\mathbf{s} = \mathbf{e}_\theta + \mathbf{e}_\Omega \quad (62)$$

Combining Eqs.(48, 61, 62), one has

$$\begin{aligned} \dot{\mathbf{s}} = & H\mathbf{e}_\theta - k_4 \mathbf{e}_\theta + \dot{e}_{\zeta_\theta} + f(\boldsymbol{\Omega}) + \\ & g(\boldsymbol{\Omega})\boldsymbol{\Sigma} + D_3 - \dot{\boldsymbol{\Omega}}_d \end{aligned} \quad (63)$$

The sliding mode surface approach law is written as^[25]

$$\dot{\mathbf{s}} = -\epsilon \operatorname{sgn}(\mathbf{s}) - k_5 \mathbf{s} \quad (64)$$

where $\epsilon > 0$ is designed parameter, and $k_5 = k_5^T > 0$ the designed symmetric positive definite matrix.

The control law of attitude acquisition subsystem is designed as follows

$$\begin{aligned} \boldsymbol{\Sigma}^* = & g(\boldsymbol{\Omega})^{-1}(-f(\boldsymbol{\Omega}) + \dot{\zeta}_\theta - H\mathbf{e}_\theta + \\ & k_4 \mathbf{e}_\theta - \dot{D}_3 - \epsilon \operatorname{sgn}(\mathbf{s}) - k_5 \mathbf{s}) \end{aligned} \quad (65)$$

Considering Eqs.(63—65), one has

$$\dot{\mathbf{s}} = \dot{\zeta}_\theta - \dot{\boldsymbol{\Omega}}_d - \dot{D}_3 - \epsilon \operatorname{sgn}(\mathbf{s}) - k_5 \mathbf{s} + \dot{e}_{\zeta_\theta} \quad (66)$$

In order to avoid system chattering caused by the sign function vector, the smooth function vector $\boldsymbol{\gamma}_1(\mathbf{s})$ is used to approximate $\operatorname{sgn}(\mathbf{s})$, and the expression is as follows^[21]

$$\boldsymbol{\gamma}_1(\mathbf{s}) = \frac{\mathbf{s}}{\|\mathbf{s}\| + \mu_1} \quad (67)$$

where $\mu_1 > 0$ is the design parameter. Defining the difference between the sign function vector and the smooth function vector, then we have $\boldsymbol{\gamma}_0 = \operatorname{sgn}(\mathbf{s}) - \boldsymbol{\gamma}_1(\mathbf{s})$. Since the symbolic function vector and the smooth function vector are bounded, $\boldsymbol{\gamma}_0$ sat-

isfies that $\|\boldsymbol{\gamma}_0\| \leq \bar{\boldsymbol{\gamma}}_0$ is the unknown positive constant. Therefore, the modified control law of the attitude subsystem can be obtained as

$$\boldsymbol{\Sigma} = \mathbf{g}(\boldsymbol{\Omega})^{-1}(-\mathbf{f}(\boldsymbol{\Omega}) + \dot{\boldsymbol{\zeta}}_{\boldsymbol{\Omega}} - \mathbf{H}\mathbf{e}_{\boldsymbol{\Omega}} + k_4\mathbf{e}_{\boldsymbol{\theta}} - \hat{\mathbf{D}}_3 - \boldsymbol{\varepsilon}\boldsymbol{\gamma}_1(s) - k_5s) \quad (68)$$

The Lyapunov function is designed as

$$\mathbf{V}_6 = 0.5s^T s + 0.5\mathbf{e}_{\zeta_{\theta}}^T \mathbf{e}_{\zeta_{\theta}} + 0.5\mathbf{e}_{\zeta_{\Omega}}^T \mathbf{e}_{\zeta_{\Omega}} \quad (69)$$

Considering Eqs.(57, 58, 66, 69), we have

$$\begin{aligned} \dot{\mathbf{V}}_6 &\leq -s^T k_5 s - s^T \bar{\mathbf{D}}_3 - s^T (\mathbf{e}_{\zeta_{\theta}}/\mu_{\theta} + \dot{\boldsymbol{\Theta}}_d) - \\ &\boldsymbol{\varepsilon}s^T \boldsymbol{\gamma}_0 - s^T (\mathbf{e}_{\zeta_{\Omega}}/\mu_{\Omega} + \dot{\boldsymbol{\Omega}}_d) + \mathbf{e}_{\zeta_{\theta}}^T (-\mathbf{e}_{\zeta_{\theta}}/\mu_{\theta} - \dot{\boldsymbol{\Theta}}_d) + \\ &\mathbf{e}_{\zeta_{\Omega}}^T (-\mathbf{e}_{\zeta_{\Omega}}/\mu_{\Omega} - \dot{\boldsymbol{\Omega}}_d) \leq -s^T (k_5 - (1.5 + 0.5\boldsymbol{\varepsilon} + \\ &1/\mu_{\theta} + 1/\mu_{\Omega})\mathbf{I}_3) s + 0.5\|\bar{\mathbf{D}}_3\|^2 - \\ &(0.5/\mu_{\theta} - 0.5)\mathbf{e}_{\zeta_{\theta}}^T \mathbf{e}_{\zeta_{\theta}} + \bar{\boldsymbol{\Omega}}_d^2 + 0.5\boldsymbol{\varepsilon}\bar{\boldsymbol{\gamma}}_0^2 + \\ &\bar{\boldsymbol{\Theta}}_d^2 - (0.5/\mu_{\Omega} - 0.5)\mathbf{e}_{\zeta_{\Omega}}^T \mathbf{e}_{\zeta_{\Omega}} \end{aligned} \quad (70)$$

3 Stability Analysis

Based on the system model and the control objectives in section 1, and the controller design in section 2, the following theorem is given.

Theorem 1 For the unmanned HSLs in Eq.(8) with the limited load swing angle and external disturbances, the nonlinear disturbance observer (21) of the slung-load subsystem, the constrained robust controller (31) of the slung-load subsystem based on the error transfer function, the nonlinear disturbance observer (36) of the velocity subsystem and the robust controller (45) of the slung-load subsystem are designed. As well as the nonlinear disturbance observer (48) of the attitude subsystem and the sliding mode backstepping controller (68), the signals of the closed-loop system are ultimately uniformly bounded, and the load swing angle meets the prescribed performance (11).

Proof The Lyapunov function of the closed-loop system is constructed as

$$\begin{aligned} \mathbf{V} &= \mathbf{V}_1 + \mathbf{V}_2 + \mathbf{V}_3 + \mathbf{V}_4 + \mathbf{V}_5 + \mathbf{V}_6 = \\ &0.5\bar{\mathbf{d}}_1^T \bar{\mathbf{d}}_1 + 0.5\boldsymbol{\omega}_1^T \boldsymbol{\omega}_1 + 0.5\boldsymbol{\omega}_2^T \boldsymbol{\omega}_2 + \\ &0.5\bar{\mathbf{D}}_2^T \bar{\mathbf{D}}_2 + 0.5\mathbf{e}_r^T \mathbf{e}_r + 0.5\bar{\mathbf{D}}_3^T \bar{\mathbf{D}}_3 + \\ &0.5s^T s + 0.5\mathbf{e}_{\zeta_{\theta}}^T \mathbf{e}_{\zeta_{\theta}} + 0.5\mathbf{e}_{\zeta_{\Omega}}^T \mathbf{e}_{\zeta_{\Omega}} \end{aligned} \quad (71)$$

According to Eqs.(25, 34, 40, 46, 53, 70), one has

$$\begin{aligned} \dot{\mathbf{V}} &= -\boldsymbol{\omega}_1^T \mathbf{k}_1 \boldsymbol{\omega}_1 - \boldsymbol{\omega}_2^T \mathbf{k}_2 \boldsymbol{\omega}_2 - \mathbf{e}_r^T \mathbf{k}_3 \mathbf{e}_r - \mathbf{e}_r^T \bar{\mathbf{D}}_2 + \\ &s^T [-\boldsymbol{\varepsilon}(\boldsymbol{\gamma}_0 + \boldsymbol{\gamma}_1(s)) - k_5 s - \bar{\mathbf{D}}_3 + \dot{\mathbf{e}}_{\zeta_{\theta}} + \dot{\mathbf{e}}_{\zeta_{\Omega}}] + \\ &\boldsymbol{\omega}_2^T \bar{\mathbf{d}}_1 + \mathbf{e}_{\zeta_{\theta}}^T \dot{\mathbf{e}}_{\zeta_{\theta}} + \mathbf{e}_{\zeta_{\Omega}}^T \dot{\mathbf{e}}_{\zeta_{\Omega}} \leq -\boldsymbol{\kappa}\mathbf{V} + c \end{aligned} \quad (72)$$

where

$$\begin{aligned} \boldsymbol{\kappa} &= 2\lambda_{\min}\{\mathbf{k}_1, \mathbf{k}_2 - 0.5\mathbf{I}_2, \mathbf{k}_3 - 0.5\mathbf{I}_3, \mathbf{k}_5 - (1.5 + \\ &0.5\boldsymbol{\varepsilon} + 1/\mu_{\theta} + 1/\mu_{\Omega})\mathbf{I}_3, L_1 - \mathbf{I}_2, L_2 - \mathbf{I}_3, L_3 - \mathbf{I}_3, \\ &0.5/\mu_{\theta} - 0.5, 0.5/\mu_{\Omega} - 0.5\} \\ c &= 0.5\delta_1^2 + 0.5\delta_2^2 + 0.5\boldsymbol{\varepsilon}\bar{\boldsymbol{\gamma}}_0^2 + \bar{\boldsymbol{\Theta}}_{\boldsymbol{\Omega}}^2 + \bar{\boldsymbol{\Theta}}_{\boldsymbol{\Omega}}^2 + \bar{\boldsymbol{\Xi}}_d^2 \end{aligned}$$

It can be known from Eq.(72) that the three controllers (31, 45, 68) designed for the unmanned HSLs can ensure all signals of the closed-loop system bounded. Then, we have

$$\mathbf{V} \leq \frac{\boldsymbol{\kappa}}{c} + \left[\mathbf{V}(0) - \frac{\boldsymbol{\kappa}}{c} \right] e^{-c t} \quad (73)$$

Considering Eq.(73), the following conclusion can be drawn that the system signal $\boldsymbol{\omega}_1, \boldsymbol{\omega}_2, \mathbf{e}_r, s, \mathbf{e}_{\zeta_{\theta}}$ and $\mathbf{e}_{\zeta_{\Omega}}$ are ultimately uniformly bounded. It can be obtained

$$\frac{1}{2}\|\boldsymbol{\beta}\|^2 = \frac{1}{2}\|\boldsymbol{\omega}_1\|^2 \leq \frac{\boldsymbol{\kappa}}{c} + \left[\mathbf{V}(0) - \frac{\boldsymbol{\kappa}}{c} \right] e^{-c t} \quad (74)$$

According to Eq.(74), when the time $t \rightarrow \infty$, the signal $\boldsymbol{\beta}$ will meet $\|\boldsymbol{\beta}\| \leq \sqrt{2\boldsymbol{\kappa}/c}$. Then the tracking error of hoisting subsystem can meet the preset performance in Eq.(11). Similarly, other signals $\boldsymbol{\omega}_2, \mathbf{e}_r, s, \mathbf{e}_{\zeta_{\theta}}$ and $\mathbf{e}_{\zeta_{\Omega}}$ are also bounded, so the theorem is proved.

4 Simulation Results and Analysis

To verify the effectiveness of the designed controller, the medium-sized unmanned helicopter is selected as the simulation research object in this section. Specific simulation parameters are as follows: The unmanned helicopter model quality $m_h = 1000$ kg, the slung-load quality $m_l = 100$ kg, the length of the rope $l = 10$ m, the gravitational acceleration $g = 9.8$ m/s², the triaxial moment of inertia $J_{xx} = 180$ kg·m², $J_{yy} = 200$ kg·m² and $J_{zz} = 220$ kg·m², the equivalent damping coefficient of the load $k = 0.2$, the external disturbances are assumed to be that $\mathbf{d}_1 = [\sin 10t + \cos 10t, \sin 10(t+1) + \cos 10(t+1)]^T$, $\mathbf{D}_2 = [\cos 10t, \cos 10(t+1), \cos 10(t+2)]^T$, and $\mathbf{D}_3 = [\sin 10t, \sin 10(t+1), \sin 10(t+2)]^T$. The performance function of

hoisting subsystem is selected as $\chi_1(t) = 0.4\exp(-4t) + 0.01$, $\chi_2(t) = 0.3\exp(-4t) + 0.01$. Assume that the system is in a low-speed flat flight state, and the flight speed of the unmanned helicopter is $[u_d, v_d, w_d]^T = [10, 5, 2]^T$, $\dot{w}_d = 0$. The load stability swing angles can be obtained by balancing $[\theta_{ld}, \phi_{ld}]^T \approx [0.15 \text{ rad}, 0.08 \text{ rad}]^T$.

After full debugging, the controller parameters are set as $\lambda_1 = \lambda_2 = 0.5$, $k_1 = \text{diag}\{25, 20\}$, $k_2 = \text{diag}\{15, 15\}$, $k_3 = 1000I_3$, $k_4 = 50$, $\varepsilon = 5$, $k_5 = 10I_3$, $\mu_\theta = \mu_\alpha = 0.1$, $u_1 = 5$, $L_1 = 80I_3$, $L_2 = 100I_3$, $L_2 = 120I_3$.

The simulation results are shown in Figs.2—11. Fig.2 shows that the two swing angles θ_1 and ϕ_1 of the slung-load can be stabilized quickly to the ideal swing angles of 0.15 rad and 0.08 rad under the action of the designed backstepping controller. The prescribed performance of the two tracking errors

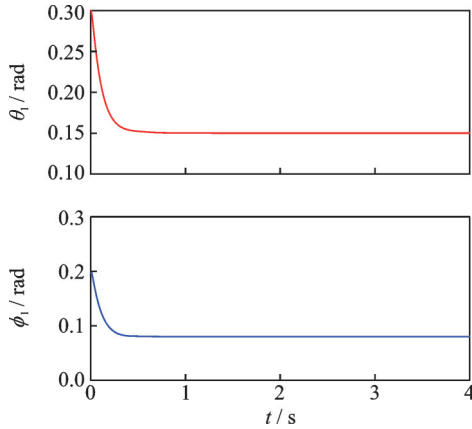


Fig.2 Curves of slung-load angle

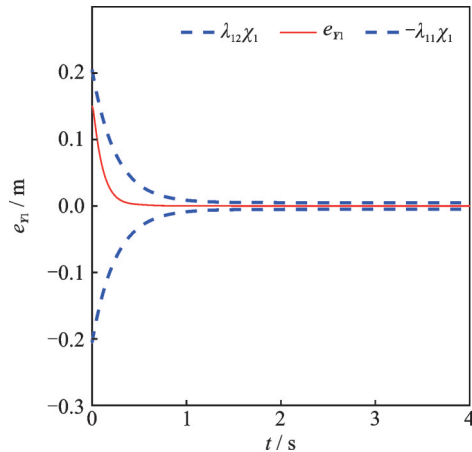


Fig.3 Error of e_{y1} with prescribed performance

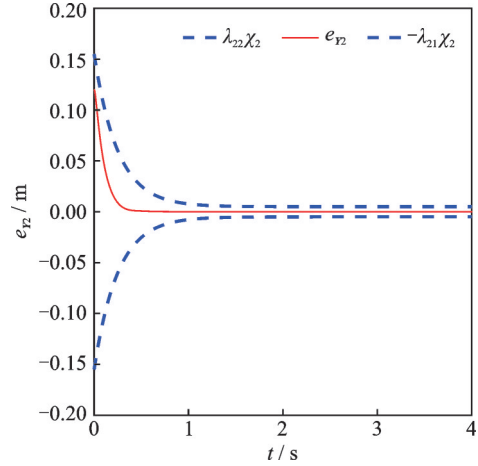


Fig.4 Error of e_{y2} with prescribed performance

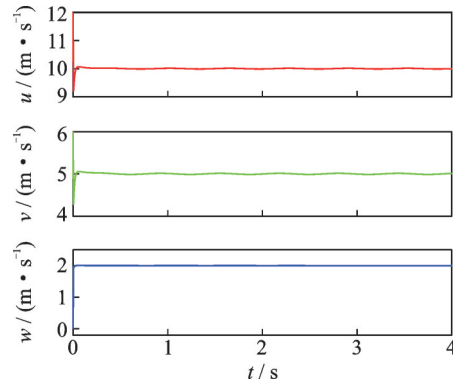


Fig.5 Tracking curves of unmanned helicopter speed

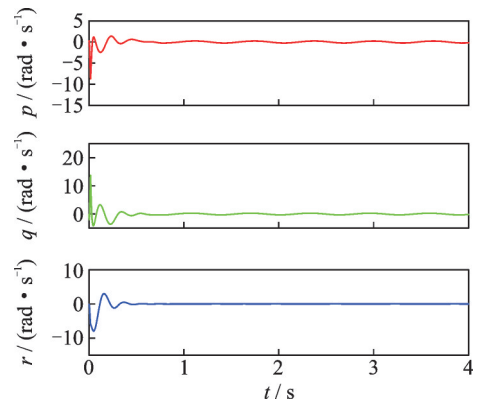


Fig.6 Curves of unmanned helicopter angular velocity

e_{y1} and e_{y2} of slung-load swing angles are fully reflected in Fig.3 and Fig.4, respectively, and it can be seen that the transient and steady-state performance of tracking errors can be guaranteed by adjusting the parameters of the prescribed performance function. From Figs.5—7, the designed robust controller (45) of the speed subsystem and the robust controller of the attitude subsystem controller (68) have good control performance, and the system

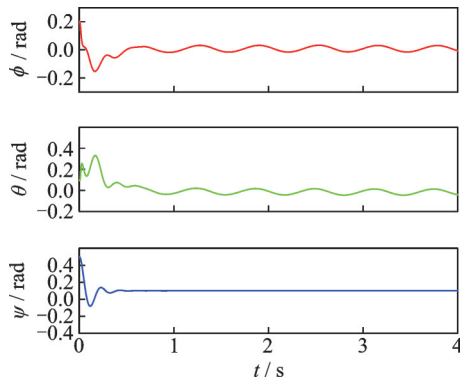


Fig.7 Curves of unmanned helicopter Euler angle

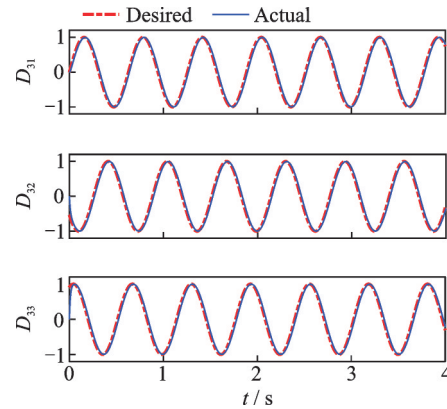


Fig.10 Tracking curves of disturbance observer in attitude subsystem

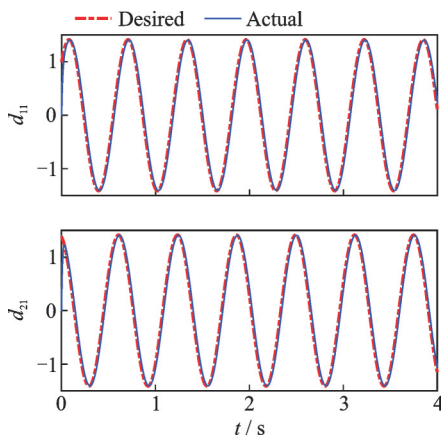


Fig.8 Tracking curves of disturbance observer in slung-load subsystem

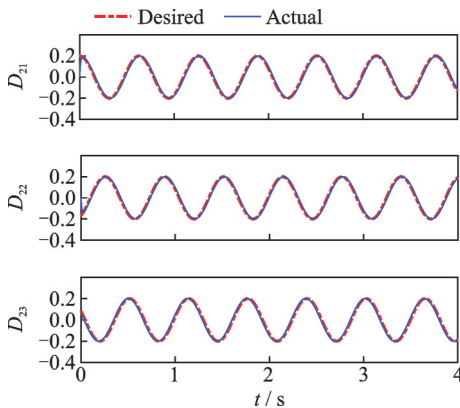
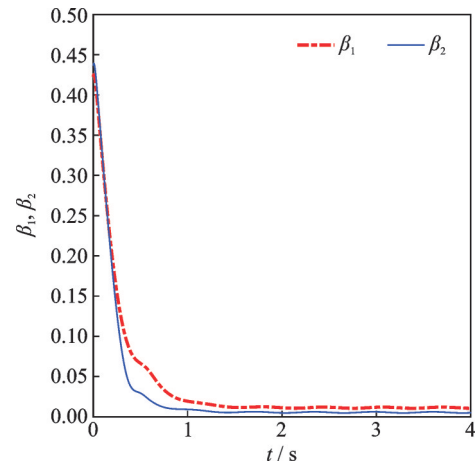


Fig.9 Tracking curves of disturbance observer in speed subsystem

state of the unmanned helicopter can quickly converge to the target values. The estimation performance of the disturbance observers (21, 36, 49) are shown in Figs. 8—10. We can see that the designed disturbance observers can quickly estimate the actual disturbances, and the estimation error is stable within a small range. Furthermore, the transfer error variables β_1 and β_2 are also convergent, as

Fig.11 Curves of transfer error variables β_1 and β_2

shown in Fig. 11. In conclusion, the simulation results verify the effectiveness of the designed control method.

5 Conclusions

The damping control of the coupling nonlinear unmanned HSLs in the lifting process has been studied. Two ideal swing angles of the slung-load under the flat flight for the unmanned helicopter have been obtained off-line. Considering the disturbance of the slung-load subsystem, a prescribed robust controller of load swing angles have been constructed to ensure that the load can converge quickly and be stabilized near the ideal swing angles with the anti-disturbance ability. Aiming at the speed and attitude subsystem subject to external disturbance, the robust controllers have been designed for the speed and the attitude of the unmanned helicopter based on the disturbance observer. Then the stabili-

ty of the closed-loop system is proved by constructing the Lyapunov function. Finally, the simulation results show that the designed control scheme can achieve the expected control goal. In the future research, the robust anti-swing control based on the neural networks will be studied for the unmanned helicopter slung-load system with system uncertainties.

References

- [1] QI Wantao, CHEN Renliang. Stability and control characteristic analysis for flight of helicopter with slung load[J]. *Journal of Nanjing University of Aeronautics and Astronautics*, 2011, 43(3): 406-412. (in Chinese)
- [2] WU Peng, MA Chengjiang, ZHU Guomin. Flight dynamics modeling and handling quality analysis of helicopter with slung-load[J]. *Helicopter Technique*, 2010, 25(4): 33-36. (in Chinese)
- [3] CHEN Yuan, CHEN Renliang. Coupling analysis of helicopter flying with slung load[J]. *Journal of Nanjing University of Aeronautics and Astronautics*, 2017, 49(2): 165-172. (in Chinese)
- [4] CAO Yihua, WANG Zhaorui. Equilibrium characteristics and stability analysis of helicopter slung-load coupling system[J]. *Journal of Beijing University of Aeronautics and Astronautics*, 2014, 40(9): 1219-1224. (in Chinese)
- [5] WANG Shaofeng, CAO Yihua, HUANG Lei. Dynamic modeling of helicopter-flexible rope-slung load system based on Kane's method[J]. *Journal of Aerospace Power*, 2016, 31(4): 934-940. (in Chinese)
- [6] WANG Haining. Decreasing oscillations of aerial cranes[D]. Beijing, China: Beijing Institute of Technology, 2015. (in Chinese)
- [7] BI Mengyue. Research on controllability stability analysis and control method for helicopter-slung load coupling system[D]. Nanjing: Nanjing University of Aeronautics and Astronautics, 2018. (in Chinese)
- [8] MO R, GENG Q, LU X. An active disturbance rejection controller design and parameter tuning for helicopter with slung-load[C]//*Proceedings of 2016 12th IEEE International Conference on Control and Automation (ICCA)*. Nepal: IEEE, 2016.
- [9] EL-FERIK S, SYED A H, OMAR H M, et al. Nonlinear forward path tracking controller for helicopter with slung load[J]. *Aerospace Science & Technology*, 2017, 69(1): 602-608.
- [10] HE Rongrong, CHEN Mou, WU Qingxian, et al. Sliding mode backstepping anti-swing control of helicopter slung-load system[J]. *Aero Weaponry*, 2019, 41(8): 1-10. (in Chinese)
- [11] EL-FERIK S, SYED A H, OMAR H M, et al. Anti-swing nonlinear path tracking controller for helicopter slung load system[J]. *IFAC Proceedings Volumes*, 2013, 46(30): 134-141.
- [12] WANG Shizhang, XIAN Bin, YANG Sen. Anti-swing controller design for an unmanned aerial vehicle with a slung-load[J]. *Acta Automatica Sinica*, 2018, 44(10): 1771-1780. (in Chinese)
- [13] SUN Ning, FANG Yongchun, WANG Pengcheng, et al. Adaptive trajectory tracking control of underactuated 3-dimensional overhead crane systems[J]. *Acta Automatica Sinica*, 2010, 36(9): 1287-1294. (in Chinese)
- [14] XIONG Ying, CHEN Mou, WU Qingxian, et al. Robust tracking control of variable swept-wing near space vehicle based on disturbance observers[J]. *Science China: Information*, 2019, 49(5): 585-598. (in Chinese)
- [15] JIA Z, YU J, MEI Y, et al. Integral backstepping sliding mode control for quadrotor helicopter under external uncertain disturbances[J]. *Aerospace Science and Technology*, 2017, 68(10): 299-307.
- [16] CHEN M, CHEN W. Sliding mode control for a class of uncertain nonlinear system based on disturbance observer[J]. *Control Signal Process*, 2010, 24(13): 51-64.
- [17] ZHANG Z, WANG F, GUO Y, et al. Multivariable sliding mode backstepping controller design for quadrotor UAV based on disturbance observer[J]. *Science China Information Sciences*, 2018, 61(15): 1-16.
- [18] CHEN M, REN B, WU Q, et al. Anti-disturbance control of hypersonic flight vehicles with input saturation using disturbance observer[J]. *Science China Information Sciences*, 2015, 58(3): 1-12.
- [19] TEE K P, GE S S, TAY E. Barrier Lyapunov functions for the control of output-constrained nonlinear systems[J]. *Automatica*, 2009, 45(27): 918-927.
- [20] IICHMANN A, SCHUSTER H. PI-funnel control for two mass systems[J]. *IEEE Transactions on Automatic Control*, 2009, 54(4): 918-923.
- [21] YAN K, CHEN M, WU Q. Neural network-based adaptive fault tolerant tracking control for unmanned autonomous helicopters with prescribed performance[J]. *Journal of Aerospace Engineering*, 2019, 233(12): 4350-4362.
- [22] YANG H, JIANG B, YANG H, et al. Synchroniza-

tion of multiple 3-DOF helicopters under actuator faults and saturations with prescribed performance[J]. ISA Transactions, 2018, 75(1): 118-126.

- [23] WANG C, YANG G. Observer-based adaptive prescribed performance tracking control for nonlinear systems with unknown control direction and input saturation[J]. Neurocomputing, 2018, 284(1): 17-26.
- [24] HE Yuebang, PEI Hailong, YE Xiang, et al. Adaptive dynamic surface trajectory tracking control for unmanned helicopter[J]. South China University of Technology Scientific Journal (Natural Science edition), 2013, 41(5): 1-8. (in Chinese)
- [25] CHEN Zhi. Robust sliding mode control theory and its application in unmanned helicopter[D]. Nanjing: Nanjing University of Aeronautics and Astronautics, 2017. (in Chinese)

Acknowledgements This work was supported in part by the National Natural Science Foundation of China (No. 62003163), the National Science Fund for the Key R & D projects (Social Development) in Jiangsu Province of China (No. BE2020704), the Aeronautical Science Foundation of China (Nos. 201957052001, 20200007052001), the Jiangsu Province “333” project (No. BRA2019051), the Postdoctoral Research Foundation of Jiangsu Province (No. 2020Z112), and the Natural Science Foundation of Jiangsu Province for Young Scholars (No. BK20200415).

Authors Dr. SHAO Shuyi received his M. S. degree in control theory and control engineering from Nanjing Normal University, Nanjing, China, in 2014, and Ph.D. degree in control theory and control engineering from the College of Automation Engineering, Nanjing University of Aeronautics and Astronautics, Nanjing, China, in 2019. From March

2017 to September 2017 and March 2018 to March 2019, he was a visiting scholar with the Department of Mechanical, Industrial and Aerospace Engineering, Concordia University, Montreal, Quebec, Canada. His research interests include fractional-order nonlinear system control, applications of chaos synchronization, and flight control.

Prof. CHEN Mou received his B.S. degree in material science and engineering and Ph.D. degree in control theory and control engineering from Nanjing University of Aeronautics and Astronautics (NUAA), Nanjing, China, in 1998 and 2004, respectively. He is currently a full professor at the College of Automation Engineering, NUAA. He was an academic visitor at the Department of Aeronautical and Automotive Engineering, Loughborough University, Loughborough, U.K., from November 2007 to February 2008. From June 2008 to September 2009, he was a research fellow at the Department of Electrical and Computer Engineering, National University of Singapore. He was a senior academic visitor at the School of Electrical and Electronic Engineering, University of Adelaide, Adelaide, Australia, from May 2014 to November 2014. His research interests include nonlinear system control, intelligent control, and flight control.

Author contributions Dr. SHAO Shuyi conducted the analysis, interpreted the results and wrote the manuscript. Mr. LIU Nan contributed to the discussion and background of the study, and wrote the manuscript. Ms. LI Chunru contributed to the discussion of the study, and proofread the manuscript. Prof. CHEN Mou designed the study and revised the paper. All authors commented on the manuscript draft and approved the submission.

Competing interests The authors declare no competing interests.

(Production Editor: ZHANG Bei)

无人直升机吊装系统预设性能鲁棒减摆控制

邵书义^{1,2}, 刘楠¹, 李春茹¹, 陈谋¹

(1.南京航空航天大学自动化学院, 南京 211106, 中国; 2.南京航空航天大学航空学院, 南京 210016, 中国)

摘要:针对无人直升机吊装系统在吊运过程中受扰而偏离平衡态的问题,研究了一种基于误差转换函数的鲁棒减摆控制方法。首先建立无人直升机吊装系统的全状态耦合非线性数学模型;其次利用平飞下无人直升机吊装系统的两个理想摆角值和实际摆角值构造了摆角误差,并且研究误差变换函数以保证摆角误差满足预设性能;然后引入非线性干扰观测器估计有界干扰,并且分别基于预设性能方法、干扰观测器的输出和滑模反演方法设计无人直升机吊装系统的鲁棒控制器、速度和姿态子系统的鲁棒控制器;进一步利用构造的李雅普诺夫函数证明了闭环系统稳定性;最后仿真结果表明了控制策略的有效性。

关键词:无人直升机吊装系统;预设性能;减摆控制;干扰观测器;滑模控制器